

Micromechanical modelling of the arterial wall: influence of mechanical heterogeneities on the wall stress distribution and the peak wall stress

M. Toungara^{a*}, L. Orgéas^a, C. Geindreau^a and L. Bailly^b

^aCNRS, University of Grenoble, Laboratoire 3SR, BP 53, 38041, Grenoble Cedex 9, France; ^bCNRS, Aix-Marseille University, IRPHE, 13384 Marseille, France

Keywords: abdominal aortic aneurysm; wall stress; anisotropy; heterogeneous mechanical properties

1. Introduction

Previous tensile tests have shown the high anisotropy and heterogeneity of the arterial wall mechanical properties as a function of age, pathology (e.g. abdominal aortic aneurysm, AAA) and location (Vande Geest et al. 2006). The issues of this anisotropic behaviour and the AAA geometrical shapes have been tackled in many numerical studies. However, the wall mechanical heterogeneity has been very sparsely considered (Tierney et al. 2012). This work aims to study the effects of such heterogeneity on the stress distribution and the peak wall stress during a static pressurisation. Thence, a micromechanical-based model was used for the wall, and finite element analyses (FEA) were carried out on idealised AAAs. Unlike many previous phenomenological models, the current constitutive model depends on five material parameters only, which also allow us to control the wall microarchitecture.

2. Methods

2.1 Micromechanical model

The arterial wall was idealised as two lattices (I and II), each comprising two families of straight fibres, embedded in an incompressible neo-Hookean soft membrane. The lattice (Figure 1(a)) can be seen as a repetition of a representative elementary cell (REC) as sketched in Figure 1(b). Let us note $\mathbf{p}_{0i} = \ell_{0i}\mathbf{E}_i$ and $\mathbf{p}_i = \ell_i\mathbf{e}_i$, the fibre vectors in the initial (\mathcal{R}_0) and deformed (\mathcal{R}) configurations, respectively. In \mathcal{R}_0 (respectively in \mathcal{R}), the fibre i has a length ℓ_{0i} (respectively ℓ_i) and is oriented along the unit vector \mathbf{E}_i (respectively \mathbf{e}_i), making angles θ_{0i}^I (respectively θ_i^I) and θ_{0i}^{II} (respectively θ_i^{II}) with the orthoradial direction \mathbf{e}_θ of the wall. The tension in a fibre i is defined as $\mathbf{t}_i = c_0(\ell_i/\ell_{0i})\{\exp[c_1/2((\ell_i/\ell_{0i})^2 - 1)] - 1\}\mathbf{e}_i$, where c_0 and c_1 are material parameters. From the REC

and its micromechanics, the homogenisation provides the macroscopic Cauchy' stress tensor

$$\boldsymbol{\sigma} = \boldsymbol{\sigma}_m + \frac{1}{h_0\|\mathbf{p}_1 \wedge \mathbf{p}_2\|} \sum_{i=1}^2 \mathbf{t}_i \otimes \mathbf{p}_i + \frac{1}{h_0\|\mathbf{p}_3 \wedge \mathbf{p}_4\|} \sum_{i=3}^4 \mathbf{t}_i \otimes \mathbf{p}_i,$$

where $\boldsymbol{\sigma}_m$ is the stress tensor of the soft membrane and h_0 an arbitrary thickness. The second and third terms in the right side correspond to the first (I) and the second (II) lattices (Bailly et al. 2012).

2.2 Microstructure optimisation

Each microstructure parameter was adjusted with biaxial tensile data (Vande Geest et al. 2006). An optimisation process based on a least-squares approach was used. The parameters identified on average data (26 AAA samples and 8 AA samples, mean age: 70 ± 4) are summarised in Table 1. Details of the discrepancies between experimental and optimised data are reported in Bailly et al. (2012).

2.3 Geometrical model

Idealised AAAs were built in SolidWorks[®], using a mathematical form as in Toungara et al. (2012). These AAAs were characterised by the dilatation parameter ($R_{an}/R_a = 2.75$), the eccentricity ($F_e = e/(R_{an} - R_a)$) and the aspect ratio ($L_{an}/R_{an} = 2.50$), with $R_a = D/2 = 10$ mm the AA radius, R_{an} the AAA maximum radius and L_{an} the AAA length. The shift of R_{an} from the AA axis is defined by e . For sake of simplicity, a uniform and

*Corresponding author. Email: mamadou.toungara@3sr-grenoble.fr

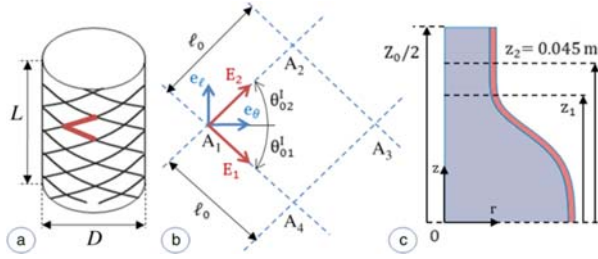


Figure 1. (a) Lattice I, (b) in-plane view of the REC in \mathcal{R}_0 and (c) geometry of an axisymmetric AAA ($F_e = 0$). When $|z| \geq z_2$, the artery is assumed to be healthy; the artery total length $Z_0 = 0.1$ m.

Table 1. Model parameters for AA (healthy aorta) and AAA tissues.

	c_0 (N)	c_1	θ_0^I ($^\circ$)	θ_0^{II} ($^\circ$)	ℓ_0 (mm)
AA	0.00140	37.99	31	60	5.0
AAA	0.00076	70.73	27	56	5.0

constant wall thickness (1.50 mm) was adopted. Figure 1 (c) shows an example of an axisymmetric AAA ($F_e = 0$).

2.4 Mechanical heterogeneity

Pathological and healthy material parameters were considered in the bulged ($0 \leq |z| \leq z_1$) and the straight ($z_2 \leq |z| \leq Z_0/2$) regions of the artery (see Figure 1(c) and Table 1), respectively. A linear evolution of these parameters was proposed in the AA–AAA transitional zone ($z_1 \leq |z| \leq z_2$). Thereafter, owing to lack of experimental data, the width of this zone was parametrically varied: $z_1 \in [0, z_2]$.

2.5 Numerical simulations

The above material model was implemented in Comsol Multiphysics[®] by which FEA were carried out. U-P formulation was adopted with Lagrangian P2-P1 finite elements. A typical structured mesh was adopted in this study. At both proximal and distal ends of the artery, the axial displacement was set to zero, whereas the radial displacement was free. Finally, the mean systolic pressure (120 mmHg) was applied at the inner side of the AAA.

3. Results and discussion

The distribution and the peak of the first principal stress, σ_1 and $\sigma_{1\max}$, was analysed as a function of the AAA eccentricity (F_e) and the width of the AA–AAA transitional zone.

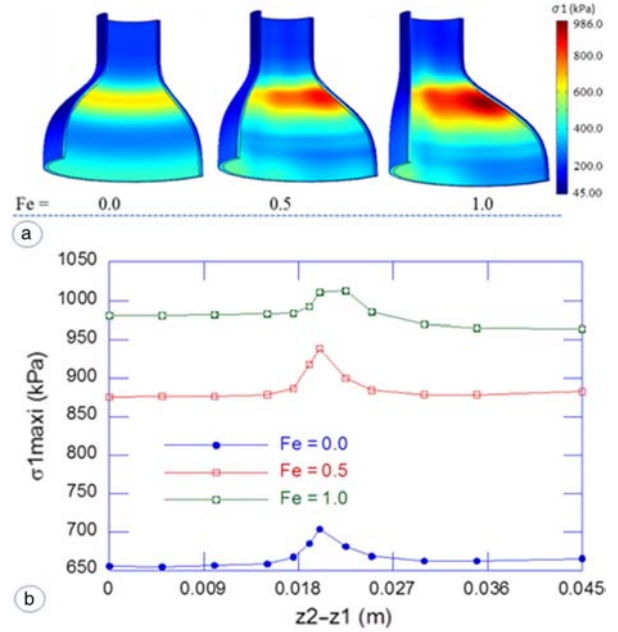


Figure 2. (a) First principal stress (σ_1) distribution in homogeneous wall and (b) heterogeneous wall, influence of AA–AAA transitional zone on $\sigma_{1\max}$.

3.1 Homogeneous AAA wall

When the AAA material parameters were adopted for the whole artery, $\sigma_{1\max}$ is observed in the proximal/distal region of the artery (Figure 2(a)). This maximum is localised in the anterior region of the AAA when the latter is asymmetric ($F_e \neq 0$). Moreover, $\sigma_{1\max}$ increases with the increase of eccentricity: $\sigma_{1\max}$ (kPa) = {655, 876, 986} for $F_e = \{0.0, 0.5, 1.0\}$. In the same way, when the AA material parameters were considered for the whole artery, $\sigma_{1\max}$ (kPa) = {719, 965, 1031} for $F_e = \{0.0, 0.5, 1.0\}$, resulting in an increase of 5–10% in $\sigma_{1\max}$. Previously, using a phenomenological material model for the AAA wall, we had obtained $\sigma_{1\max} = 1655$ kPa for the most asymmetric AAA (Toungara et al. 2012). In that case, the material model was stiffer than that used here. However, the value of $\sigma_{1\max}$ in this study is still very close to the average ultimate stress (1019 kPa) observed in uniaxial tensile tests on AAA tissues (Raghavan et al. 1996).

3.2 Heterogeneous AAA wall

When the AA and the AAA regions are considered with proper mechanical properties and with different widths ($z_2 - z_1$) of the transitional zone, the previous stress distribution (Figure 2(a)) remains unchanged. But, from the homogeneous case, $\sigma_{1\max}$ increases by about 7% when the limit of the pathological region of the artery (z_1) is in the geometrical junction of the straight and the bulged parts (Figure 1(c)), i.e. for $z_2 - z_1 \approx 0.02$ m, whatever the

AAA eccentricity (Figure 2(b)). Similar results have been recently observed by Tierney et al. (2012). These authors considered the wall mechanical heterogeneity in patient-specific AAAs, by dividing the wall into four regions (posterior, anterior, right and left laterals), each with its own material parameters. From the homogeneous case, an increase of about 10% in $\sigma_{1\max}$ was obtained with the heterogeneous wall.

4. Conclusion

Micromechanical based anisotropic and heterogeneous model was proposed for the arterial tissue. This model was implemented in FEA software, and the wall stress distribution and the peak wall stress were computed in idealised AAAs. The preliminary results are in agreement with previous results from the literature. We also highlighted the prevalence of structural effects, versus material properties, namely the heterogeneity, on the numerical prediction of the peak wall stress. Therefore, when predicting the AAA rupture or manufacturing phantom AAAs, besides the wall mechanical properties, special caution should be paid to geometrical aspects.

Finally, let us remark that the used micromechanical model permits to consider the fibres arrangement and their mechanical behaviour. Consequently, more complex behaviour for fibres (stiffening, damage, etc.) can be readily introduced in order to predict the AAAs rupture.

References

- Bailly L, Geindreau C, Orgéas L, Deplano V. 2012. Towards a biomimetism of abdominal healthy and aneurysmal arterial tissues. *J Mech Behav Biomed Mater.* 10:151–165.
- Raghavan ML, Webster MW, Vorp DA. 1996. *Ex-vivo* biomechanical behavior of abdominal aortic aneurysm: assessment using a new mathematical model. *Ann Biomed Eng.* 24:573–582.
- Tierney AP, Callanan A, McGloughlin TM. 2012. Use of regional mechanical properties of abdominal aortic aneurysms to advance finite element modeling of rupture risk. *J Endovasc Ther.* 19:100–114.
- Toungara M, Chagnon G, Geindreau C. 2012. Numerical analysis of the wall stress in abdominal aortic aneurysm: influence of the material model near-incompressibility. *J Mech Med Biol.* 12:1250005–1250019.
- Vande Geest JP, Sacks MS, Vorp DA. 2006. The effects of aneurysm on the biaxial mechanical behavior of human abdominal aorta. *J Biomech.* 39:1324–1334.